

Assessment of different approaches for background correction in microwave plasma atomic emission spectrometry – case study for analysis of Cd, Cr, Cu, Ni, Pb and Zn in treated bio-waste

V. Y. Markova^{1,2*}, K. K. Simitchiev¹

¹Department of Analytical Chemistry and Computer Chemistry, University of Plovdiv “Paisii Hilendarski”,
24 Tzar Assen Str., 4000 Plovdiv, Bulgaria

²Laboratory for Testing of Solid Biofuels and Compost, Energy Agency of Plovdiv, 139 Ruski Blvd, office 403,
4000 Plovdiv, Bulgaria

Received November 14, 2018; Revised December 6, 2018

Several approaches for background correction were studied when nitrogen microwave plasma atomic emission spectrometry (MP-AES) was applied for analysis of Cd, Cr, Cu, Ni, Pb and Zn in treated bio-waste (compost and stabilized organic fraction samples). Since the temperature of the microwave plasma is relatively lower than that of the argon operated inductively coupled plasma, the former excitation source is more prone to the occurrence of structured background emission, as well as matrix-induced shifts at the background level. Indeed, these two effects were observed when sample solutions of the treated bio-waste were subjected to measurements by MP-AES and led to the need to investigate the adequateness of the implemented background correction algorithm. A comparison of the “on-peak”, two-sided “off-peak” and one-sided “off-peak” correction approaches was made for the following emission lines: Cd I 228.802; Cd II 226.502; Cr I 427.480; Cr I 520.844; Cu I 324.754; Cu I 327.395; Ni I 341.476; Ni I 305.082; Pb I 405.781; Pb I 363.957; Zn I 213.857; Zn I 481.053. Furthermore, the spread of wavelengths (1 or 3 CCD pixels) used for intensity integration was also evaluated. The tested correction algorithms led to different results only in the case of Ni I 305.082 and Pb I 363.957. Nevertheless, it was found that the one-sided/off-peak/3 pixels approach was adequate for all studied analyte lines. In addition, it was proved that the measurement repeatability was not influenced by the used mathematical model for background correction.

Keywords: background correction, microwave plasma atomic emission spectrometry (MP-AES), compost, stabilized organic fraction, bio-waste

INTRODUCTION

The microwave induced plasma is well known concept [1] used in elemental analysis. Commercial microwave induced plasma atomic emission spectrometer (MP-AES) has been introduced on the market since 2011 [2]. The plasma is sustained using microwave magnetic field and nitrogen, which can be extracted from the ambient air. MP-AES has been applied for the quantification of B, P and Mo in biosludge [2], trace elements in fusel oil [3], sunflower [4], leather and fur [5], gasoline and ethanol [6], animal feed and fertilizer [7], trace and macro elements in geochemical samples [8] and environmental samples [9], macro elements in soils [10], lanthanides in environmental samples [11].

The microwave plasma has different properties than the inductively coupled argon plasma, two of which are the lower temperature (around 5000 K) and the operation on nitrogen [12]. The background of the microwave plasma is reported to be highly structured due to the emission of radical species

such as NO⁺, NO, N₂, N₂⁺, NH, OH [12], which impact on the analytical signal that must be assessed. Three approaches for background correction are provided by the MP Expert software of Agilent 4200 MP-AES spectrometer: “automatic” correction, “off-peak” two-sided correction, “off-peak” one-sided correction [13]. The “automatic” correction is defined as linear regression method [12], but no information is supplied if this algorithm is able to correct a shift in the background level caused by any difference of the matrices of the standard solutions and the analysed samples. The concept of the “off-peak” correction is well known [13], but the adequateness of this approach is usually strongly dependent on the choice of the “off-peak” wavelengths, as well as the number of pixels used for integration of the signal (for spectrometers with CCD or CID).

In our previous investigations we have found that MP-AES has sufficient detection power for the determination of Cd, Cr, Cu, Ni, Pb and Zn in compost [14]. However, no detailed investigation

* To whom all correspondence should be sent.
E-mail: vzapryanova@uni-plovdiv.net

V.Y. Markova, K.K. Simitchiev: Assessment of different approaches for background correction in microwave plasma ... of the different approaches for background correction has been made. The aim of the current study was to compare and select the most appropriate algorithm for background correction needed for MP-AES analysis of Cd, Cr, Cu, Ni, Pb and Zn in treated bio-waste such as compost and stabilized organic fraction (SOF).

EXPERIMENTAL

Nitric acid ($\text{HNO}_3 \geq 65\%$, Fluka, p.a. grade) was used for extraction of soluble fractions of elements from compost and stabilized organic fraction (SOF). Ultrapure water with $2 \mu\text{S cm}^{-1}$ electroconductivity (Ultrapure Water System Adjarov Technology Ltd.) was used throughout this work for preparation of solutions and rinsing the vessels. Standard solutions were prepared from a multi-element standard solution (ICP Multi-element Standard Solution IV 1000 mg L^{-1} - Ag, Al, B, Ba, Bi, Ca, Cd, Co, Cr, Cu, Fe, Ga, In, K, Li, Mg, Mn, Na, Ni, Pb, Sr, Tl, Zn, Merck KGaA) by dilution with acidified ultrapure water (1% v/v HNO_3).

The analysed samples – compost and SOF were produced by one of the regional waste management systems in Bulgaria treating biodegradable waste. The samples were dried in an oven at 40°C for 16 hours, after that they were quartered to provide about 500 g sub-sample which was homogenized with a cutting mill Retsch SM 200.

A microwave digestion system (MARS 6, CEM Corporation) with closed vessels was used to perform the microwave-assisted extraction. The samples were proceeded in accordance with the EN 16173 [15]. The samples passed through the extraction procedure were diluted with factor 50 or 100 and blank sample was proceeded.

A nitrogen microwave induced plasma optical emission spectrometer MP-AES 4200 Agilent Technologies was used. The measured emission lines were Cd I 228.802; Cd II 226.502; Cr I 427.480; Cr I 520.844; Cu I 324.754; Cu I 327.395; Ni I 341.476; Ni I 305.082; Pb I 405.781; Pb I 363.957; Zn I 213.857; Zn I 481.053.

Multivariate optimization of the operating parameters (sample flow rate, nebulizer gas flow rate and optical view point) was carried out by using central composite design as a tool for experimental planning. The MP-AES operating parameters are presented in Table 1.

All calculations for background correction were carried out by spreadsheet program (MS Excel) using “raw” data (registered intensities at defined wavelengths), exported from the MP Expert software of the 4200 Agilent MP-AES.

Table 1. MP-AES 4200 Agilent operating parameters

| | |
|--|---------|
| Magnetron, MHz | 2450 |
| Plasma gas, L.min^{-1} | 20 |
| Auxiliary gas, L.min^{-1} | 1.5 |
| Nebulizer type | OneNeb® |
| Optics viewing position | axial |
| Integration (read) time, s | 1 |
| Number of readings | 5 |
| Nebulizer gas flow rate, L.min^{-1} | 0.65 |
| Sample flow rate, mL.min^{-1} | 1.43 |
| Optical view point | 0 |

RESULTS AND DISCUSSION

The instrumental set-up of Agilent 4200 MP-AES allows the registration of each analyte line within a spectral window of approximately 0.6 nm consisting of *ca.* 40 measurement pixels (Fig. 1). This allows the operator to assess the background near the spectral line of interest, as well as the appearance of other lines generated from interfering elements. An evaluation of the background emission within the registered spectral windows for selected wavelengths of the studied elements (Cd, Cr, Cu, Ni, Pb, Zn) have shown the structured nitrogen plasma background (Fig. 1). The latter phenomenon is due to the emission of radical species which are present in the low temperature microwave plasma [12]. In general, the existence of structured background near the analyte line is a potential obstacle for the application of the conventional “off-peak” correction approach since it becomes more sophisticated to make an adequate background subtraction. An alternative correction not influenced from the structured background is the “on-peak” approach. However, the latter mathematical method suffers from shifts of the background level among the analysed samples, e.g. the blank and the real-matrix sample. In our study, it was observed that for all studied analytical lines the background level registered for compost or SOF samples substantially drops or increases in respect to the blank solution (Fig. 1). The listed above facts show that for adequate determination of Cd, Cr, Cu, Ni, Pb and Zn in compost and SOF the applicability of the “off-peak” and “on-peak” correction approaches needs to be checked for each analyte line.

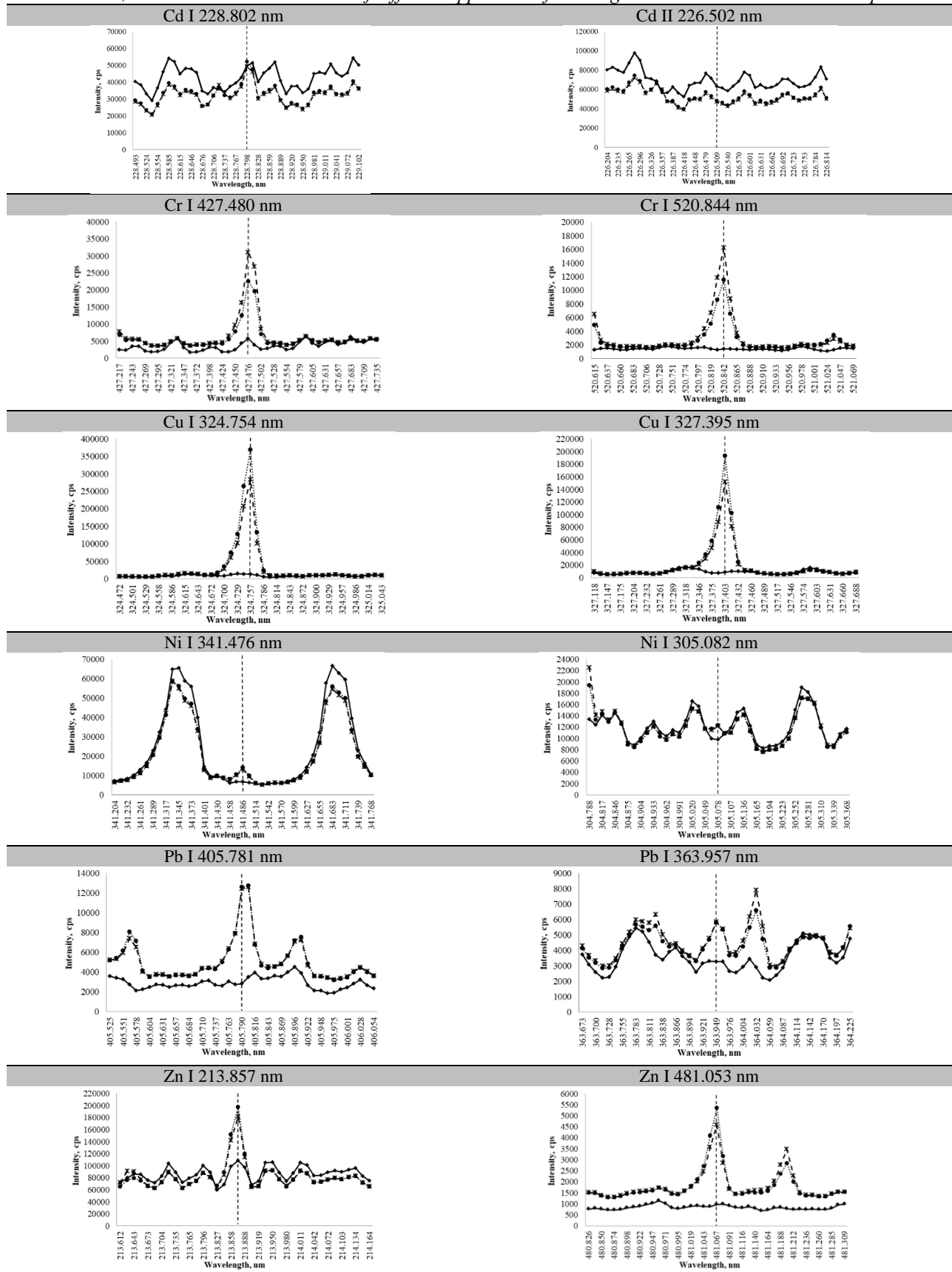


Figure 1. Profiles of the studied emission lines of elements: \rightarrow blank sample; $-*$ - compost sample with DF=100 for emission lines of Cr, Cu, Ni, Pb and Zn, and compost sample with DF=50 + 0.5 mg.L⁻¹ addition of Cd; \cdots SOF sample with DF=100 for emission lines of Cr, Cu, Ni, Pb and Zn, and SOF sample with DF=50 + 0.5 mg.L⁻¹ addition of Cd. With vertical dashed line is presented the position of WP wavelength used in eqs. 1-3.

In the current work we have studied the following algorithms for background correction: i) “on-peak” using intensities derived from bins of 1 registered pixel (Eq. 1); ii) two-sided “off-peak” using bins of 1 pixel (2 sided/off-peak/1 pixel) (Eq. 2); iii) two-sided “off-peak” using bins of 3 pixels (2 sided/off-peak/3 pixels) (Eq. 2); iv) one-sided “off-peak” using bins of 1 pixel (1 sided/off-peak/1 pixel) (Eq. 3); and v) one-sided “off-peak” using bins of 3 pixels (1 sided/off-peak/3 pixels) (Eq. 3). The “on-peak” correction was applied according to Equation 1. This approach requires the initial registration of the spectrum of the blank solution (1% v/v nitric acid) and was based on the assumption that the magnitude of any matrix-induced shift in the background level will have the same value at the analyte wavelength, as well as in the neighbor region around the spectral line of interest. At the two-sided “off-peak” correction a linear interpolation was performed between two background points (one on either side of the analyte peak) to predict the background intensity at the analyte wavelength, which is then subtracted from the analyte signal (Eq. 2). The one-sided “off-peak” correction was carried out by subtraction of the emission signal at the analyte wavelength and the intensity at selected background point located in the left or right side of the analyte peak (Eq. 3).

$$I_{corrected}^{on-peak} = I_S^{WP} - \left(\frac{I_S^{LP} + I_S^{RP}}{2} - \frac{I_B^{LP} + I_B^{RP}}{2} \right) \quad \text{Eq. 1}$$

$$I_{corrected}^{2\ sided/off-peak} = I_S^{WP} - [slope(I_S^{LP}:I_S^{RP}; LP:RP) \times WP + intercept(I_S^{LP}:I_S^{RP}; LP:RP)] \quad \text{Eq. 2}$$

$$I_{corrected}^{1\ sided/off-peak} = I_S^{WP} - I_S^{LP\ or\ RP} \quad \text{Eq. 3}$$

I_S^{WP} - the emission intensity registered at a wavelength pixel closest to the maximum of the analyte spectral peak (for on-peak; 2 sided/off-peak/1 pixel and 1 sided/off-peak/1 pixel correction) or average of a bin of 3 pixels enclosing the peak maximum (for 2 sided/off-peak/3 pixels and 1 sided/off-peak/ 3 pixels correction);

I_S^{LP} - the corresponding intensities registered for a sample solution at a pixel (for on-peak; 2 sided/off-peak/1 pixel and 1 sided/off-peak/1 pixel correction) or average of a bin of 3 pixels (for 2 sided/off-peak/3 pixels and 1 sided/off-peak/ 3 pixels correction) located in the left side of the analyte spectral peak;

I_S^{RP} - the corresponding intensities registered for a sample solution at a pixel (for on-peak; 2 sided/off-peak/1 pixel and 1 sided/off-peak/1 pixel correction) or average of a bin of 3 pixels (for 2 sided/off-peak/3 pixels and 1 sided/off-peak/ 3 pixels correction) located in the right side of the analyte spectral peak;

I_B^{LP} - the corresponding intensities registered for the blank solution at a wavelength pixel located in the left side of the analyte spectral peak (for “on-peak” correction);

I_B^{RP} - the corresponding intensities registered for the blank solution at a wavelength pixel located in the right side of the analyte spectral peak (for “on-peak” correction);

WP - the wavelength (nm) at a pixel, closest to the maximum of the analyte spectral peak;

LP - the wavelength (nm) at a pixel located in the left side of the analyte spectral peak;

RP - the wavelength (nm) at a pixel located in the right side of the analyte spectral peak.

The wavelengths at which the corresponding intensities were taken for calculation of the “on-peak”, the two-sided “off-peak” and the one-sided “off-peak” correction of the studied analyte lines are given in Table 2.

Table 2. Wavelengths at which the corresponding intensities were used for calculation of the “on-peak”, two-sided “off-peak” and one-sided “off-peak” correction using bins of 1 pixel or 3 pixels

| WP, nm | Bins of 1 pixel | | | Bins of 3 pixels | | | | |
|--------------|-----------------|---------|---------|------------------|---------|---------|---------|---------|
| | LP, nm | RP, nm | LP1, nm | LP2, nm | LP3, nm | RP1, nm | RP2, nm | RP3, nm |
| 228.802 (Cd) | 228.630 | 228.859 | 228.615 | 228.630 | 228.646 | 228.844 | 228.859 | 228.874 |
| 427.480 (Cr) | 427.398 | 427.528 | 427.385 | 427.398 | 427.411 | 427.515 | 427.528 | 427.541 |
| 520.844 (Cr) | 520.774 | 520.888 | 520.763 | 520.774 | 520.785 | 520.876 | 520.888 | 520.899 |
| 324.754 (Cu) | 324.629 | 324.943 | 324.615 | 324.629 | 324.643 | 324.929 | 324.943 | 324.957 |
| 327.395 (Cu) | 327.246 | 327.517 | 327.232 | 327.246 | 327.261 | 327.503 | 327.517 | 327.531 |
| 341.476 (Ni) | 341.458 | 341.528 | 341.444 | 341.458 | 341.472 | 341.514 | 341.528 | 341.542 |
| 305.082 (Ni) | 304.890 | 305.180 | 304.875 | 304.890 | 304.904 | 305.165 | 305.180 | 305.194 |
| 405.781 (Pb) | 405.697 | 405.935 | 405.684 | 405.697 | 405.710 | 405.922 | 405.935 | 405.948 |
| 363.957 (Pb) | 363.907 | 363.990 | 363.894 | 363.907 | 363.921 | 363.976 | 363.990 | 364.007 |
| 213.857 (Zn) | 213.796 | 213.950 | 213.781 | 213.796 | 213.811 | 213.934 | 213.950 | 213.965 |
| 481.053 (Zn) | 480.995 | 481.116 | 480.983 | 480.995 | 481.007 | 481.104 | 481.116 | 481.128 |

Table 3. Comparison of the results obtained by “on-peak”, two-sided “off-peak” and one-sided “off-peak” background correction for a) compost and b) SOF sample

| Line | LOQ, mg L ⁻¹ | on-peak | | 2 sided/off-peak/1 pixel | | 2 sided/off-peak/3 pixels | | 1 sided/off-peak/1 pixel | | 1 sided/off-peak/3 pixels | |
|--------------|----------------------------|---------------------------|------------------------|---------------------------|------------------------|---------------------------|------------------------|---------------------------|------------------------|---------------------------|------------------------|
| | | Conc., mg L ⁻¹ | SD, mg L ⁻¹ | Conc., mg L ⁻¹ | SD, mg L ⁻¹ | Conc., mg L ⁻¹ | SD, mg L ⁻¹ | Conc., mg L ⁻¹ | SD, mg L ⁻¹ | Conc., mg L ⁻¹ | SD, mg L ⁻¹ |
| a) Compost | | | | | | | | | | | |
| Cd I 228.802 | 0.02 ^f | 0.498 ^a | 0.001 | 0.495 ^a | 0.003 | 0.508 ^a | 0.002 | 0.497 ^{a,d} | 0.003 | 0.498 ^{a,d} | 0.002 |
| Cr I 427.480 | 0.02 ^f | 0.518 ^b | 0.004 | 0.518 ^b | 0.004 | 0.515 ^b | 0.004 | 0.515 ^{b,d} | 0.004 | 0.511 ^{b,d} | 0.004 |
| Cr I 520.844 | 0.03 ^f | 0.491 ^b | 0.010 | 0.491 ^b | 0.011 | 0.509 ^b | 0.011 | 0.492 ^{b,e} | 0.011 | 0.509 ^{b,e} | 0.011 |
| Cu I 324.754 | 0.007 ^f | 1.27 ^b | 0.02 | 1.27 ^b | 0.02 | 1.28 ^b | 0.02 | 1.27 ^{b,e} | 0.02 | 1.28 ^{b,e} | 0.02 |
| Cu I 327.395 | 0.009 ^f | 1.32 ^b | 0.01 | 1.32 ^b | 0.01 | 1.31 ^b | 0.01 | 1.32 ^{b,e} | 0.01 | 1.32 ^{b,e} | 0.02 |
| Ni I 341.476 | 0.05 ^f | 0.207 ^b | 0.001 | 0.207 ^b | 0.002 | 0.214 ^b | 0.001 | 0.207 ^{b,e} | 0.001 | 0.207 ^{b,e} | 0.002 |
| | | 1.19 ^c | 0.02 | 1.19 ^c | 0.02 | 1.21 ^c | 0.02 | 1.19 ^{c,e} | 0.02 | 1.19 ^{c,e} | 0.02 |
| Ni I 305.082 | 0.08 ^f | 0.222 ^b | 0.001 | 0.225 ^b | 0.003 | 0.205 ^b | 0.002 | 0.234 ^{b,e} | 0.003 | 0.216 ^{b,e} | 0.003 |
| | | 1.23 ^c | 0.01 | 1.24 ^c | 0.01 | 1.21 ^c | 0.01 | 1.25 ^{c,e} | 0.01 | 1.23 ^{c,e} | 0.01 |
| Pb I 405.781 | 0.07 ^f | 1.07 ^b | 0.02 | 1.08 ^b | 0.02 | 1.06 ^b | 0.02 | 1.09 ^{b,d} | 0.02 | 1.09 ^{b,d} | 0.02 |
| Pb I 363.957 | 0.11 ^g | 0.85 ^b | 0.01 | 0.85 ^b | 0.01 | 0.77 ^b | 0.01 | 1.05 ^{b,d} | 0.02 | 1.07 ^{b,d} | 0.01 |
| Zn I 213.857 | 0.08 ^f | 5.55 ^b | 0.02 | 5.55 ^b | 0.03 | 5.54 ^b | 0.03 | 5.50 ^{b,d} | 0.03 | 5.53 ^{b,d} | 0.03 |
| Zn I 481.053 | 0.90 ^f | 5.52 ^b | 0.03 | 5.51 ^b | 0.03 | 5.57 ^b | 0.03 | 5.52 ^{b,d} | 0.02 | 5.51 ^{b,d} | 0.03 |
| b) SOF | | | | | | | | | | | |
| Cd I 228.802 | 0.02 ^f | 0.552 ^a | 0.001 | 0.549 ^a | 0.003 | 0.561 ^a | 0.002 | 0.550 ^{a,d} | 0.003 | 0.554 ^{a,d} | 0.002 |
| Cr I 427.480 | 0.02 ^f | 0.326 ^b | 0.005 | 0.326 ^b | 0.006 | 0.325 ^b | 0.006 | 0.323 ^{b,d} | 0.006 | 0.321 ^{b,d} | 0.006 |
| Cr I 520.844 | 0.03 ^f | 0.327 ^b | 0.004 | 0.327 ^b | 0.005 | 0.341 ^b | 0.005 | 0.328 ^{b,e} | 0.005 | 0.341 ^{b,e} | 0.005 |
| Cu I 324.754 | 0.007 ^f | 1.66 ^b | 0.02 | 1.66 ^b | 0.03 | 1.66 ^b | 0.03 | 1.65 ^{b,e} | 0.03 | 1.65 ^{b,e} | 0.03 |
| Cu I 327.395 | 0.009 ^f | 1.61 ^b | 0.01 | 1.61 ^b | 0.03 | 1.61 ^b | 0.01 | 1.61 ^{b,e} | 0.01 | 1.61 ^{b,e} | 0.01 |
| Ni I 341.476 | 0.05 ^f | 0.235 ^b | 0.001 | 0.234 ^b | 0.001 | 0.238 ^b | 0.002 | 0.236 ^{b,e} | 0.002 | 0.234 ^{b,e} | 0.002 |
| | | 1.21 ^c | 0.01 | 1.21 ^c | 0.01 | 1.22 ^c | 0.01 | 1.22 ^{c,e} | 0.01 | 1.22 ^{c,e} | 0.01 |
| Ni I 305.082 | 0.08 ^f | 0.215 ^b | 0.001 | 0.218 ^b | 0.002 | 0.213 ^b | 0.002 | 0.224 ^{b,e} | 0.001 | 0.221 ^{b,e} | 0.001 |
| | | 1.20 ^c | 0.01 | 1.20 ^c | 0.01 | 1.20 ^c | 0.01 | 1.20 ^{c,e} | 0.01 | 1.21 ^{c,e} | 0.01 |
| Pb I 405.781 | 0.07 ^f | 1.09 ^b | 0.02 | 1.09 ^b | 0.03 | 1.07 ^b | 0.03 | 1.11 ^{b,d} | 0.03 | 1.10 ^{b,d} | 0.03 |
| Pb I 363.957 | 0.11 ^g | 0.81 ^b | 0.01 | 0.81 ^b | 0.02 | 0.78 ^b | 0.02 | 0.95 ^{b,d} | 0.03 | 1.00 ^{b,d} | 0.02 |
| Zn I 213.857 | 0.08 ^f | 6.83 ^b | 0.02 | 6.83 ^b | 0.03 | 6.89 ^b | 0.03 | 6.75 ^{b,d} | 0.03 | 6.86 ^{b,d} | 0.03 |
| Zn I 481.053 | 0.90 ^f | 7.04 ^b | 0.03 | 7.03 ^b | 0.03 | 6.89 ^b | 0.05 | 7.05 ^{b,d} | 0.04 | 6.79 ^{b,d} | 0.05 |

^a sample with DF=50 + 0.5 mg.L⁻¹ Cd; ^b sample with DF=100; ^c sample with DF=100 + 1.0 mg.L⁻¹ Ni; ^d left one-sided “off-peak” correction; ^e right one-sided “off-peak” correction; ^f calculated LOQ using two-sided/off-peak/1 pixel correction; ^g calculated LOQ using left one-sided/off-peak/1 pixel correction .

The five approaches for background correction were compared for registered spectra of compost and SOF samples (Table 3). Several emission lines of elements were studied. For each element were selected two lines – one priority and one alternative, except for Cd, for which only one spectral line was reasonable to be used in view of achieving the lowest possible detection limit. However, the content of Cd in both analysed sample matrices was below the established instrumental quantification limit of 0.02 mg L⁻¹. So in order to assess the different background correction approaches (Eqs. 1-3) for this element the compost and SOF sample solutions were spiked with 0.5 mg.L⁻¹ of Cd in order to produce a measurable signal for the analyte. Another element which was present in the real samples at levels close to the established LOQs (Table 3) was Ni - the found concentrations were approximately 3 times (for Ni 305.082) and 4 times (for Ni 341.476) higher than the corresponding LOQs. Even though the detection power of MP-AES was sufficient to register the native signals of Ni in the compost and SOF the adequateness of the different background correction approaches (Eqs. 1-3) was also tested for spiked samples with 1 mg L⁻¹ Ni. The latter was done aiming to assure that the measured emission intensities at the analyte WPs are with improved signal-to-noise ratio.

In the current study a tolerance limit of 5% deviation, among the analyte concentrations achieved by different approaches for background correction, as well as by using alternative spectral lines for the target elements, was accepted. Any result, which exceeds this limit, was regarded as significantly different.

For both sample types (compost and SOF) it was found that the application of all studied approaches for background correction resulted in identical concentrations when the following analyte lines were used: Cd I 228.802, Cr I 427.480, Cr I 520.844, Cu I 324.754, Cu I 327.395, Ni I 341.476, Pb I 405.781, Zn I 213.857 and Zn I 481.053 (Table 3). Furthermore, the obtained concentrations of Cr, Cu and Zn by using the listed above spectral lines (two for each element) were within the specified tolerance limit of 5%. The correction algorithms led to different results in the case of Ni I 305.082 and Pb I 363.957. It was found that only the one-sided/off-peak/3 pixels approach gives adequate results for Ni and Pb measured respectively at 305.082 and 363.957 nm in compost and SOF samples. The evident reason for the incorrect results when “two-sided” correction was used for Pb I 363.957 is the

existence of closely located line of Fe I 364.039 nm (Fig. 1). The analysis of the treated bio-waste samples spiked with 1 mg.L⁻¹ Ni showed that all algorithms for background correction applied for the line 305.082 nm lead to identical results when the analyte concentration exceeds at least 10 times the corresponding limit of quantification (Table 3).

The measurement repeatability, as a component of the comparison among the applied background corrections, was also assessed. For the purpose, the standard deviation of five instrumental readings was calculated considering that each reading was individually proceeded using a particular background correction. The obtained results are presented in Table 3. For all studied spectral lines it was found that the derived standard deviations do not depend on the chosen approach for background correction and for every single analyte line the achieved SD values were statistically identical (Table 3).

CONCLUSIONS

Summarizing the results above it can be concluded that for all studied analyte lines adequate results can be achieved if one-sided/off-peak/3 pixels correction of the background is applied. However, all investigated algorithms for assessing the background level (Eqs. 1-3) are interchangeable applicable for the regarded set of spectral lines except for Ni I 305.082 and Pb I 363.957. It is important to be mentioned that the suggested “on-peak” approach (Eq. 1) is not integrated in the MP Expert software [13] of the 4200 Agilent MP-AES and hence it must be done by an alternative spreadsheet program (e.g. MS Excel) after an export of the registered data. The latter makes difficult to apply the “on-peak” correction for routine analysis. Since the other four “off-peak” correction algorithms (Eqs. 2 and 3) can be proceeded by the MP Expert software, the readers are suggested to use them setting the corresponding WP, LP and/or RP wavelength values as depicted in Table 2.

Acknowledgements: VM and KS are grateful for financial support of Project Number DN19/9 2018 - 2020 (INISA), financed by NSF of Bulgaria. The authors also acknowledge Dr. Violeta Stefanova for the fruitful discussions and given advices, as well as T.E.A.M. Ltd. for the complimentary supplied spectrometer Agilent 4200 MP-AES at Faculty of Chemistry, University of Plovdiv.

REFERENCES

1. A.E. Croslyn, B.W. Smith, J.D. Winefordner, *Crit. Rev. Anal. Chem.*, **27**, 199 (1997)

- V.Y. Markova, K.K. Simitchiev: Assessment of different approaches for background correction in microwave plasma ...
2. V. Sreenivasulu, N. S. Kumar, V. Dharmendra, M. Asif, V. Balaram, H. Zhengxu, Z. Zhen, *Appl. Sci.*, **7**, 264 (2017).
 3. D. Araujo, T. Mcsweeney, M. Cristina, M. A. Utrera, *Curr. Anal. Chem.*, **13** 474 (2017).
 4. S. Karlsson, V. Sjöberg, A. Ogar, *Talanta*, **135**, 124 (2015).
 5. Y. Zhao, Z. Li, A. Ross, Z. Huang, W. Chang, K. Ou-Yang, Y. Chen, C. Wu, *Spectrochim. Acta - Part B, At. Spectrosc.*, **112**, 6 (2015).
 6. G. L. Donati, R. S. Amais, D. Schiavo, J. A. Nóbrega, *J. Anal. At. Spectrom.*, **28**, 755 (2013)
 7. W. Li, P. Simmons, D. Shrader, T. J. Herrman, S.Y. Dai, *Talanta*, **112**, 43 (2013).
 8. B. Vysetti, D. Vummiti, P. Roy, C. Taylor, C. T. Kamala, M. Satyanarayanan, P. Kar, K. S. V. Subramanyam, A. K. Raju, K. Abburi, *At. Spectrosc.*, **35**, 65 (2014).
 9. C. T. Kamala, V. Balaram, M. Dharmendra, V. Satyanarayanan, K. S. V. Subramanyam, A. Krishnaiah, *Environ. Monit. Assess.*, **186**, 7097 (2014).
 10. P. Niedzielski, L. Kozak, K. Jakubowski, W. Wachowiak, J. Wybieralska, *Plant Soil Environ.*, **62**, 215 (2016).
 11. E. Varbanova, V. Stefanova, *Ecology & Safety*, **9**, 362 (2015).
 12. G. B. Partridge, *J. Anal. At. Spectrom.*, **32**, 1988 (2017).
 13. MP Expert Help, Software version 1.4.0.4317, Agilent Technologies.
 14. V. Y. Zapryanova, K. K. Simitchiev, *Bulg. Chem. Commun.*, **49 G**, 10 (2017).
 15. EN 16173 Sludge, treated biowaste and soil - Digestion of nitric acid soluble fractions of elements, 2012.